A COMPARISON OF HIGH SPATIAL RESOLUTION IMAGES FOR FINE SCALE VEGETATION MAPPING

by

Christine West

A Thesis

Presented to

The Faculty of Humboldt State University

In Partial Fulfillment

Of the Requirements for the Degree

Masters of Science

In Natural Resources: Forestry

December, 2007

ABSTRACT

A Comparison of High Spatial Resolution Images for Fine Scale Vegetation Mapping

Christine A. West

Recent advances in airborne and spaceborne sensors have made high spatial ($\leq$1m/pixel) and spectral resolution images (e.g. IKONOS, SPOT 5, Quickbird 2) widely available, raising questions regarding their utility for floristic identification and classification. Additionally, the use of object-oriented software to perform automated classification and mapping has increased throughout the past 20 years. Studies assessing the utility of these image and software options frequently center on large, homogeneous sites and do not address these applications to small, heterogenous areas typical of the Pacific Northwest. In this study, a high-density sampling grid was used (approximately 9.0 % sample), followed by agglomerative cluster analysis and ordination, to identify all vegetation alliances and associations on a 148-ha study site in Maple Creek, California. Supervised classification using object-oriented software was performed on three images of various high spatial resolutions (0.15 m 4-band aerial photo, 0.60 m 4-band satellite image, and 1 m 3-band satellite image). The resulting classifications were compared with the reference vegetation map (derived from plot and image data) to assess accuracy. Results show differences in classification accuracy between the 3 images with the 0.60m Quickbird image producing the highest overall accuracy (69%); followed by the 0.15m aerial photo (48%); and the 1m NAIP image (37%) when assessed at the alliance level.

ACKNOWLEDGEMENTS

First and foremost I thank my advisor, Dr. John Stuart, for his generosity with his time, his patience with my questions, and his diplomatic style of telling me when I was wrong. I also want to thank my committee members Dr. Larry Fox and Dr. Steven Steinberg for their guidance and encouragement. I thank my field assistant, Jasper Peach, for his hard work and tolerance of poison oak. Many thanks to Jenny Kaufmann for sharing her expertise in GIS. My appreciation to Jeffrey M. Kane for his astute editing and encouragement to push myself further. I thank George Pease for his help with field equipment and Gayleen Smith for administrative assistance. Finally, I thank Gordon Schatz for sharing his time and extensive knowledge of site history. This research was funded by the L.W. Schatz Demonstration Tree Farm.

TABLE OF CONTENTS

TABLE OF CONTENTS (CONTINUED)

LIST OF TABLES

LIST OF FIGURES

LIST OF APPENDICES

1. Introduction

The use of remote sensing technology in vegetation classification and mapping has increased over the past 30 years (Environmental Systems Research Institute and The Nature Conservancy, 1994; Jensen, 2000; Greenberg et al., 2006). Remote classification reduces the need for field sampling and alleviates access constraints, making this technology a valuable tool for resource managers (Mullerova, 2004; Leckie et al., 2005; Johansen et al., 2007). Historically, remotely-based vegetation classification was performed via manual polygon mapping with air photos (Anderson et al., 1976; Hall, 2003; Sandmann and Lertzman, 2003) as these images offered distinctly higher spatial resolution or smaller pixel sizes (Benson and MacKenzie, 1995; Lillesand et al., 2004) than satellite imagery. Recent advances in spaceborne sensors, however, have made high spatial and spectral resolution satellite images (e.g. IKONOS, SPOT 5, Quickbird 2) widely available, raising questions regarding their utility for floristic identification and classification (Carleer and Wolff, 2004; Johansen et al., 2007). Additionally, vegetation mapping methods have expanded with the development of automated classification procedures which provide image enhancement and processing techniques not available with manual mapping practices (Lillesand et al., 2004).

Higher spectral resolution, or larger number of bands in a given sensor (Lefsky and Cohen, 2003), provides opportunities for discerning vegetation characteristics unobservable in natural color (Lefsky and Cohen, 2003; Lillesand et al., 2004). The very near infrared band, in particular, allows for the development of vegetation indices such as a normalized difference (NDVI) to assist in live canopy detection (Asner et al., 2003). Higher band numbers, however, may increase scene 'noise' and image variance (Lillesand et al., 2004).

Although higher spatial resolution imagery (≤1 m) allows for clearer visualization of ground features (Lefsky and Cohen, 2003; Wulder et al., 2004) an increase in pixel number raises the internal variability within homogeneous land cover units, causing difficulties in class discernment (Carleer and Wolff, 2004). Intra-class variability issues are particularly problematic for per-pixel classifiers which rely solely on spectral signature values (Cushnie, 1987; Woodcock and Strahler, 1987; Lefsky and Cohen, 2003). Per-pixel software limitations, such as 'salt and pepper' effects where individual pixels are classified differently from their neighbors (Yu et al., 2006), have led many interpreters to believe these classifiers are not ideal for large heterogeneous units such as vegetation classes (Song et al., 2005; Yu et al., 2006). Exploration into spectral mixture analysis (Foody and Mathur, 2006) and object-oriented software, however, have shown promise in tolerating certain levels of variability (Yu et al., 2006) previously found to be problematic for per-pixel classifiers.

Consequently, object-oriented approaches have become popular for vegetation classification particularly when using higher-resolution images (Hay et al., 2005; Chubey et al., 2006). Object-based classifiers use aggregated groups of pixels, or image objects, to train the program to identify discrete entities normally recognizable to the human eye (Hay et al., 2005). In general, these programs group spatially adjacent pixels into spectrally homogeneous objects to then be used as minimum classification units

(Yu et al., 2006). Feature Analyst 4.1 (Visual Learning Systems, 2006) is a popular object-oriented commercial software package in use today that utilizes an artificial neural network classifier (Ripley, 1996) to consider spatial attributes, such as spatial association and image texture, when performing automated feature extraction (Vanderzanden and Morrison, 2003). Object-oriented classifications do not, however, always reach the commonly recommended 80 - 85% accuracy standard (Environmental Systems Research Institute and The Nature Conservancy, 1994; Congalton and Green, 1999; Foody, 2002; USDA, 2002) especially when analyzing fine scale, floristically-based categories (e.g. alliance or association). Thus, automated software users often broaden their class scales to reach this accuracy standard, resulting in coarser, homogeneous units that may not adequately reflect the heterogeneity typical of many second-growth forests (Spies et al., 1994; Jiang et al., 2004).

Furthermore, because access and sampling issues are magnified in larger areas, studies assessing the utility of remotely-driven classification frequently center on extensive sites such as entire national forests or parks (Jiang et al., 2004; Greenberg et al., 2006; Yu et al., 2006), or large private holdings (Spies et al., 1994). Limited ground sampling in these large areas for training and validation purposes (Environmental Systems Research Institute and The Nature Conservancy, 1994; Jiang et al., 2004; Leckie et al., 2005) generally results in low-confidence reference data (Foody, 2002). In this study, however, the small scale of the site afforded a unique opportunity for comprehensive ground coverage and generation of high-confidence reference information.

In addition to image resolution and classification method considerations, image type (air photo vs. satellite) may play a role in accuracy (Lefsky and Cohen, 2003). Satellite images avoid many of the problems associated with aerial photography such as join lines in mosaicked scenes, non-standardized flight orientations, or difficulty in acquiring multidate data sets (Lefsky and Cohen, 2003; Chubey et al., 2006). Spaceborne platforms can be limited, nonetheless, by inflexibility of satellite orbit schedules, as well as increased atmospheric effects due to greater sensor-to-ground distance (Lefsky and Cohen, 2003). Perhaps one of the chief issues regarding image type is the associated cost incurred with each of these options. When dealing with a small site, the price per acre of imagery may be increased as there are frequently minimum area requirements for scene purchases. Acquiring timely aerial photographs can also be prohibitively expensive due to the cost of chartering flights. Commercial satellite imagery ranges in price from \$1 – 22/km^2 (Yildirim and Seker, 2004) however government subsidized programs such as Landsat and NAIP (National Agricultural Imagery Program) offer free imagery.

There are numerous decisions land managers need to make when selecting appropriate methods for classifying vegetation such as: type of image (air photo vs. satellite), image resolution (spatial and spectral), and mapping method (automated vs. manual). These decisions need to be made in the context of the manager's objectives (e.g. habitat mapping vs. timber inventory). Research assessing these image and software options will provide land managers with information regarding the utility of using high-resolution imagery coupled with object-oriented classification software when attempting to classify vegetation. The specific objectives of this study were to (1) classify and map vegetation on a small, heterogeneous forested landscape, (2) compare the accuracy of a visual and field-based classification method with an object oriented classification method (Feature Analyst), and (3) compare the accuracy of classifying vegetation using three high spatial resolution (0.15, 0.60, and 1.0 m) digital images.

2. Materials and methods

2.1. Study area

This study was conducted on the L.W. Schatz Demonstration Tree Farm located in Maple Creek, California (Fig. 1). The 148-hectare site extends from 40°46’49’’ N to 40°45’56’’ N latitude and 123°52’21’’ W to 123°51’32’’ W longitude (T 5N, R 3E, Section 32). It ranges in elevation from 140 to 430 m, and is underlain by the Franciscan Formation, a subduction complex consisting of accreted fragments of oceanic crust and forearc sediments (Aalto and Harper, 1989).

Originally consisting of old-growth *Pseudotsuga menziesii* forest, the land was logged in the early 1950’s (Schatz 2007, personal communication). It has since experienced a mixture of natural recovery and management resulting in a heterogeneous landscape mosaic typical of many northwestern forests today (Halpern and Spies, 1995).

Current vegetation includes more than 150 species (Appendix A) and is dominated by a *P. menziesii* and mixed hardwood overstory with an understory of abundant evergreen shrubs and ferns. In addition to the forested areas, the study site contains upland prairie and a transmission right-of-way where both native and non-native perennial grasses dominate.

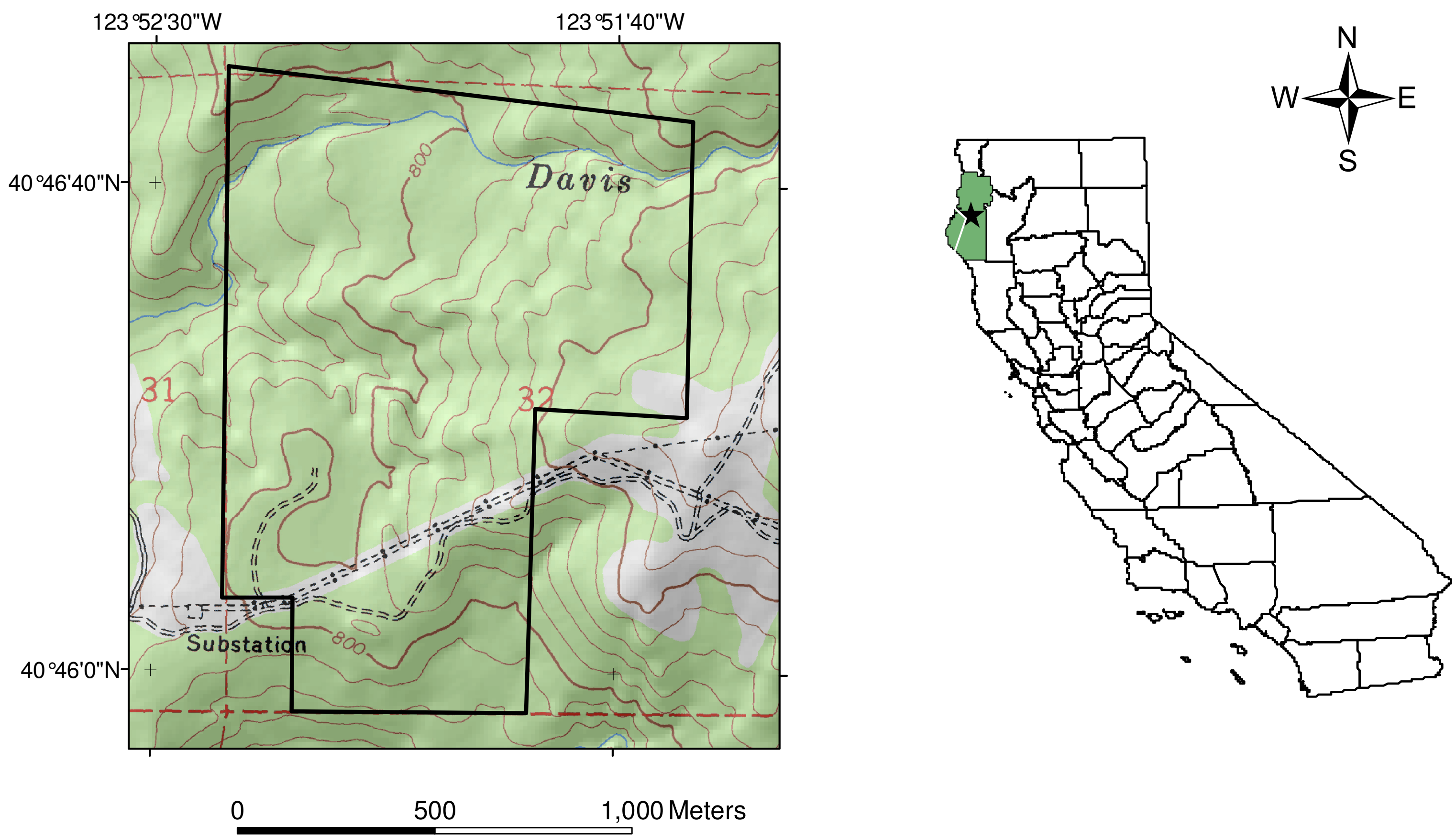

Figure 1. Location and extent of study area (outlined in black) consisting of most of the W ½ of Section 32 (T 5N, R3E), 17 miles east of Eureka, California.

2.2. Field sampling of vegetation

A high-density sampling grid scheme of 2 plots per hectare was chosen to achieve sufficient and balanced coverage of vegetation types (Cooper et al., 2006). A circular plot shape was employed for all non-riparian plots. Rectangular plots were used in riparian corridors to characterize floral composition accurately (California Native Plant Society, 2004). The maximum number of plots based on 2/ha was 296. However, the number sampled was 274 after eliminating plots overlapping the property boundary and those occurring on landslides and overly steep terrain. Two hundred and forty-eight plots were on upland, tree-dominated terrain (0.05 ha, 12.6 m radius); 8 plots were in riparian zones (0.05 ha, various dimensions); and 18 plots were in shrub- or herb-dominated areas (0.02 ha, 8.0 m radius). The plots covered approximately 9% of the tree farm.

Field data were collected from June-August, 2006 using a modified rapid assessment protocol (California Native Plant Society, 2004). Vegetation was sampled using relevé plots and modified Braun-Blanquet cover abundance scaling (Table 1; Braun-Blanquet, 1932; Lee, 2004). Ocular estimates of plant cover by species (within plot or outside of plot but providing cover within the plot) were recorded for all strata, as were average height (m) and total percentage cover by stratum (Mueller-Dombois and Ellenberg, 1974). Abiotic information recorded included: elevation (m), topographic position/landform, percent slope, aspect, and soil type (Colwell, et al., 1960).

Table 1. Cover abundance scale used in ocular estimates (Lee, 2004).

Cover Class	Cover Range (%)
1	0.001 – 0.01
2	0.01 – 0.1
3	0.1 – 1
4	1 – 5
5	5 - 15
6	15 – 25
7	25 – 50
8	50 – 75
9	75 - 100

2.3. Classification and Ordination

Vegetation data were analyzed using several multivariate approaches. Species with less than 1% total cover on the site were removed *a priori* to prevent outlier effects (McCune and Grace, 2002). Riparian plots were included in the overall analysis due to similarities in dominant vegetation with non-riparian units. Data were grouped into possible plant associations using a hierarchical clustering algorithm (Euclidean distance, Ward's linkage method) contained in PC_ORD (McCune and Grace, 2002). This method merges individual plots into groups based on species similarity. Resultant groups were then pared down through indicator analysis. Data were further analyzed via comparisons of species abundance and constancy within and between groups. A Nonmetric Multidimensional Scaling ordination was performed to further reduce the data set and graphically depict ecological relationships among plots.

The naming convention in *A Manual of California Vegetation* (Sawyer and Keeler-Wolf, 1995) was used when assigning plots to alliance and associations. Dominant species were defined as those having ≥ 50% relative cover and frequency across all plots within a vegetation type.

2.4. Image Acquisition and Processing

Three images were acquired for analysis (Fig. 2). One multispectral, 4-band (0.45 – 0.90 μm) airborne image with 0.15 m spatial resolution was acquired on June 22, 2006 for use in reference map creation and automated feature extraction. A multispectral,

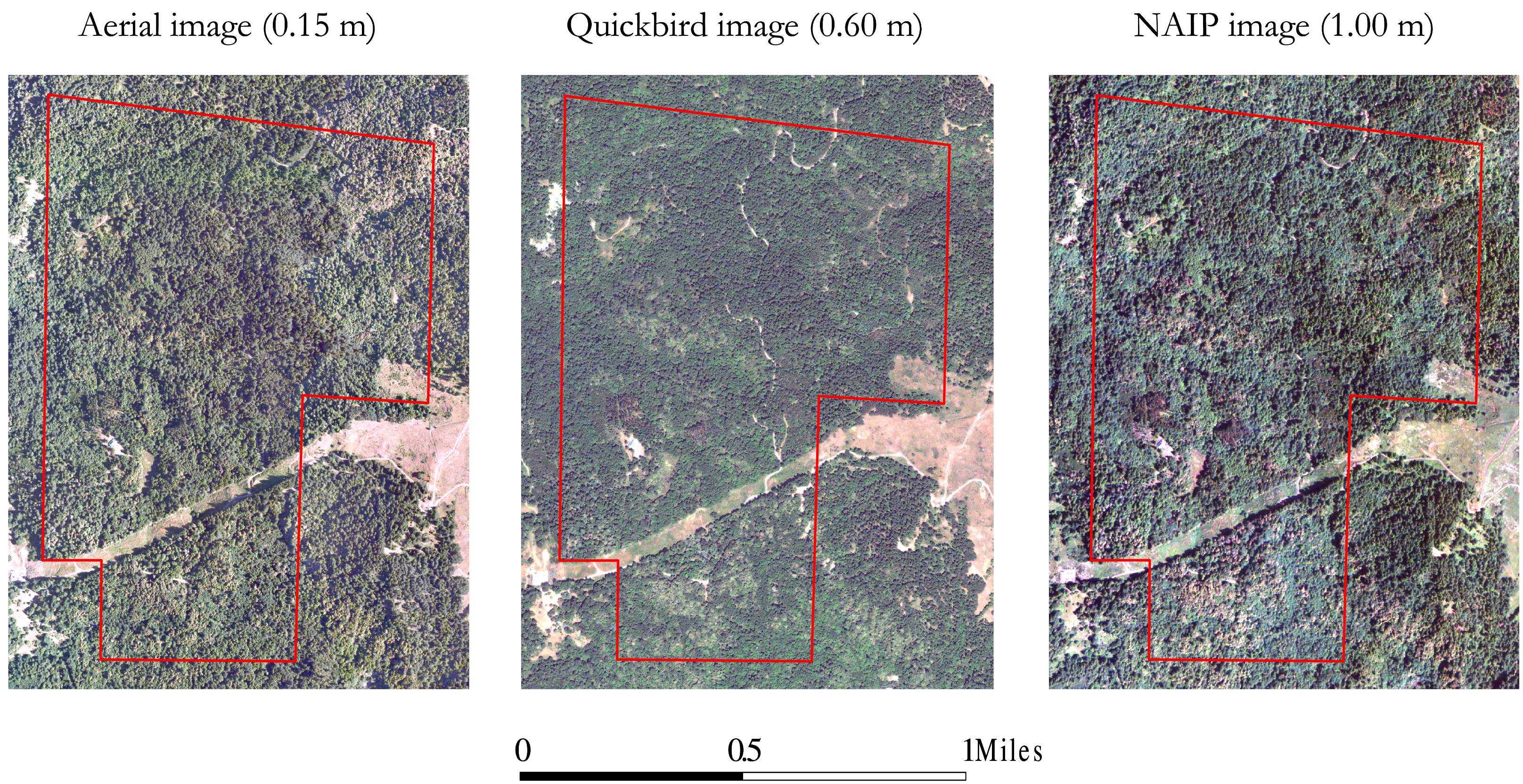

Figure 2. Digital images (and associated pixel resolution) used in analysis. Aerial image acquired on June 22, 2006, Quickbird image acquired July 28, 2006, NAIP image acquired June 15, 2005. The outline of the study site appears in red.

4-band (0.45 – 0.90 µm) QuickBird satellite image of 0.6m spatial resolution acquired July 28, 2006 by Digital Globe, and a natural color 3-band (0.45 – 0.69 µm) NAIP 1 m spatial resolution aerial image acquired June 15, 2005 by U.S. Department of Agriculture Farm Services Agency were used in automated feature extraction only.

The QuickBird image was orthorectified in ArcMap using a 10 m digital elevation model and rational polynomial coefficients (Barbarella et al., 2004). All other images were georeferenced and orthorectified by the provider. Image radiances were not atmospherically corrected (Lillesand et al., 2004) as times series analysis of consecutive image data was not required for this study and detailed information on the atmospheric conditions at the time of overpass was not available.

2.5. Vegetation Mapping

Vegetation polygons were visually interpreted and digitized in ArcMap using the 0.15 m resolution aerial image and labeled to alliance and association. The minimum mapping unit (MMU) was 1000 m^2 (approximately 2 tree-dominated ground plots) and was chosen in order to retain detail while capturing stand-level characteristics (Stohlgren et al., 1997). Vegetation polygons were laid over the remaining two images and adjusted to account for shifts in images due to error, orthorectification or georeferencing limitations. Polygons not containing at least one ground plot were verified in the field.

2.6. Automated Feature Extraction

Supervised classification of imagery was performed via automated feature extraction using Feature Analyst (Visual Learning Systems 2006) software. Training polygons were randomly selected from the reference map using Spatial Analyst in ArcGIS 9.1 to a standard of 5 or fewer polygons (approximately 40%) per vegetation type. All vegetation classes were included in association-based classification. Vegetation classes covering < 1% of the study area or those with only one polygon were masked in the alliance-based classification. Selected input parameters included pre-aggregation to 500 pixels and a representation pattern appropriate for stand-level classes (Fig. 3; Vanderzanden and Morrison, 2003). All vegetation data were used in map validation.

One classification using all available spectral bands was executed with the association reference map. Several classifications were executed with the alliance reference map. Band selection methods for alliance map analyses included: use of all available spectral bands, removal of the VNIR band in the Quickbird and aerial images, application of an NDVI to the Quickbird and aerial images, and application of only the spectral bands exhibiting the best average separability as determined by a transformed divergence statistic (Swain and Davis, 1978; ERDAS IMAGINE, 2005). Overall, the greater the transformed divergence, the greater the statistical distance between training classes and the higher the probability of correct classification (Lillesand et al., 2004). In general, if a result is greater than 1,900 then the classes can be separated; between 1,700 and 1,900 the separation is fairly good. Below 1,700 the separation is poor (Jensen, 2000).

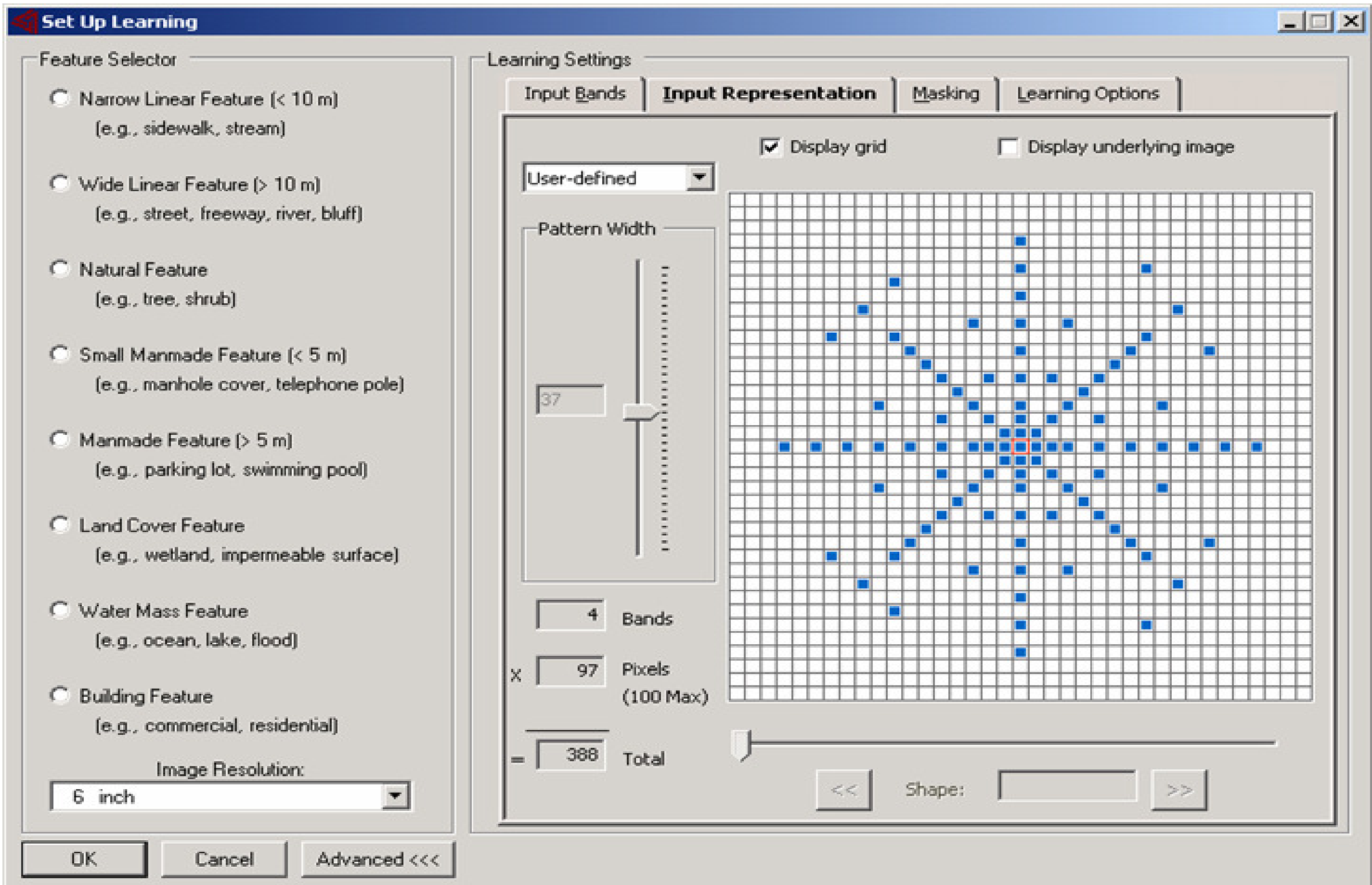

Figure 3. Feature Analyst input pattern representation. Pixels shown in blue represent those included in analysis.

To keep spatial resolution constant and test for an effect from the infrared band, the Quickbird and aerial images were resampled to 1m, and all images were run with all available spectral bands.

2.7. Accuracy Assessment

Correct vs. incorrectly classified polygons were identified in the output maps using zonal statistics in Spatial Analyst (Environmental Systems Research Institute, 2006). If the majority of pixels in the output polygon matched the reference polygon then the entire polygon was identified as correct. A majority assessment rule was chosen to account for the inherent heterogeneity within vegetation classes (Sawyer and Keeler-Wolf, 1995) and because more traditional (per-pixel) assessments of classification accuracy are often inappropriate for use in these systems (Yu et al., 2006).

Map accuracies are presented in the form of an 'error matrix' which includes measures of producer's, user's, and overall accuracy (Story and Congalton, 1986; Foody, 2002). Producer's accuracy, or error of omission, indicates the probability of a reference sample being correctly classified by the software. User's accuracy, or error of commission, indicates the probability that a pixel classified on the map represents that category on the ground (Congalton and Green, 1999). Kappa coefficients, K_{hat}, were calculated for overall map accuracy to compensate for random chance agreement (Rosenfield and Fitzpatrick-Lins, 1986).

3. Results

Twenty-five vegetation associations (Table 2; Fig. 4) and 13 vegetation alliances were classified (Table 3; Fig. 5) and mapped. *Sequoia sempervirens* plantations were included as classes in the association map as they were subcanopy dominant. *Pinus* sp. plantations were included as classes in the alliances as they were canopy dominant. The study site is primarily dominated by *P. menziesii - Abies grandis, Alnus rubra,* and *P. menziesii - Lithocarpus densiflorus* classes. Species richness per alliance varied from a low of four in a *Baccharis pilularis* alliance to a high of 21 in a *Fraxinus latifolia* riparian alliance (Table 3).

The output association maps (Fig. 6) had very low overall accuracies across all images. The Quickbird output had the highest overall accuracy (14%), followed by the NAIP (11%), and the air photo (3%). When using only 3 bands per image (R, G, B) the Quickbird output accuracy decreased to 3% while the air photo output accuracy increased to 7%.

Output maps of alliances (Fig. 7) had much higher overall accuracies across image types (Table 4) than association output maps. The Quickbird output was most accurate (69%, $K_{hat} = 0.43$), followed by air photo (48%, $K_{hat} = 0.33$), and lastly NAIP (37%, $K_{hat} = 0.28$) when all available bands were included in the analysis (Table 4, column a). The air photo and Quickbird alliance maps decreased in overall accuracy after removal of the infrared spectral band (Table 4, column b). Analyses using bands with the highest spectral separation had mixed results. The Quickbird and air photo accuracies decreased while the NAIP accuracy increased by 4% (Table 4, column c).

Table 2. Relative cover, frequency, and species richness of associations.

Associations	Relative cover (%)	Number of polygons	Mean species richness	Standard deviation of species richness
Umbellularia californica - Alnus rubra	12.6	16	16	5
Lithocarpus densiflorus	12.1	19	13	4
Umbellularia californica - Pseudotsuga menziesii	10.3	21	20	4
Pseudotsuga menziesii - Abies grandis	8.4	11	22	5
Lithocarpus densiflorus - Alnus rubra - Umbellularia californica	7.7	7	15	5
Pseudotsuga menzieseii/Rubus ursinus	6.9	11	19	7
Pseudotsuga menziesii/Polystichum munitum	6.5	9	20	3
Abies grandis - Pseudotsuga menziesii	6.3	15	20	4
Pseudotsuga menziesii - Lithocarpus densiflorus	6.1	12	21	6
Lithocarpus densiflorus - Umbellularia californica - Pseudotsuga menziesii	3.9	10	14	4
Alnus rubra	3.7	11	18	4
Transmission right-of-way	2.5	3	13	3
Tsuga heterophylla	2.1	1	9	3
Pseudotsuga menzieseii/Ceanothus thyrsiflorus	2.1	4	14	1
Lithocarpus densiflorus - Sequoia sempervirens	2.0	4	15	5
Pinus ponderosa	1.2	2	21	0
Introduced perennial grasslands	1.2	3	14	1
Pseudotsuga menziesii - Sequoia sempervirens	0.9	2	21	7
Acer macrophyllum	0.9	5	23	6
Fraxinus latifolia	0.7	5	21	2
Salix sp.	0.7	4	22	11
Ceanothus thyrsiflorus	0.6	3	18	2
Pinus radiata	0.3	1	24	0
Baccharis pilularis	0.1	2	4	0
Quercus garryana	0.1	1	17	0

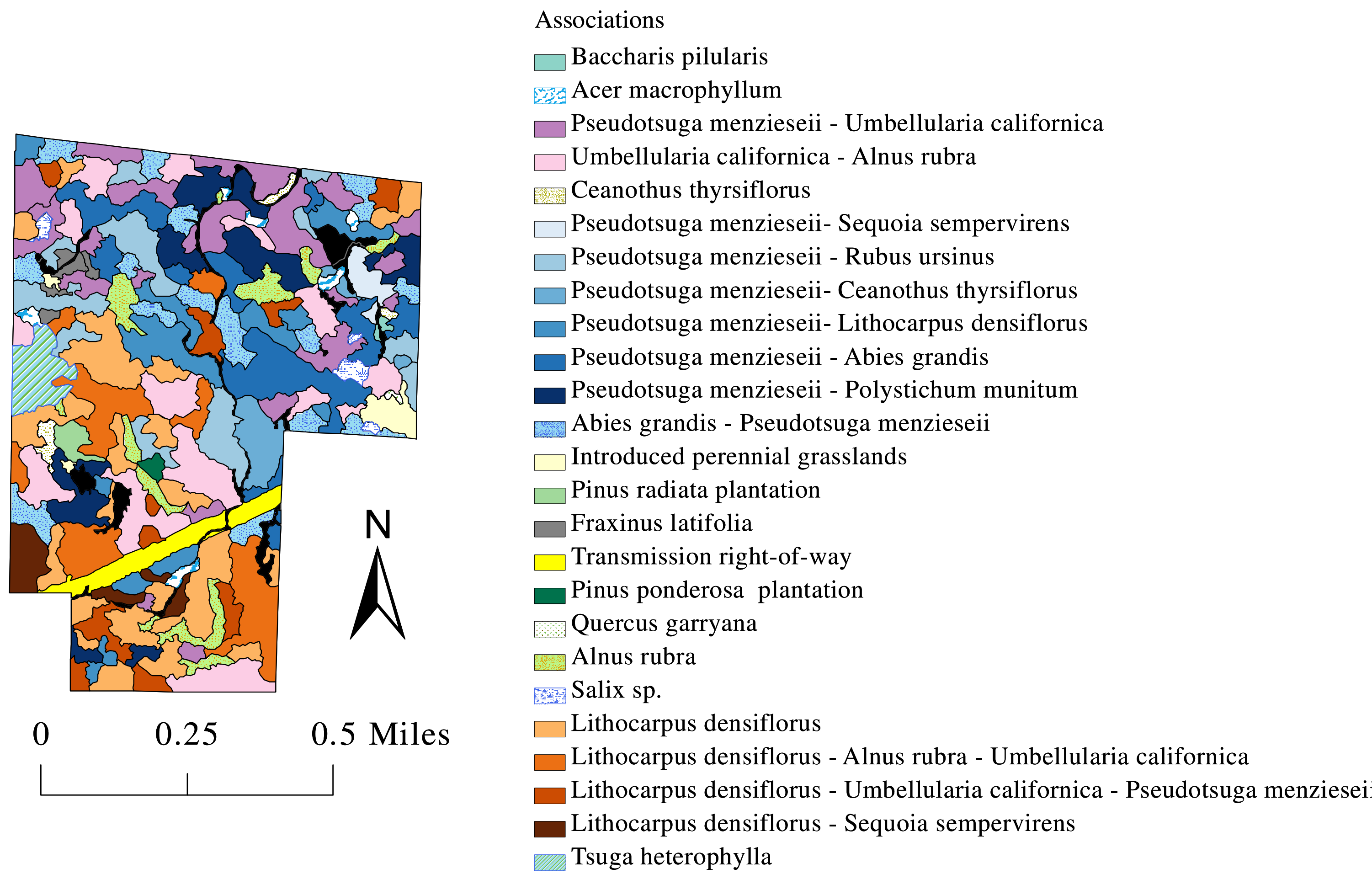

Figure 4. Thematic map showing 25 vegetative associations on study site. Areas in black were masked as non-vegetation during analysis.

Table 3. Relative cover, frequency, and species richness of alliances (*indicates vegetation classes used in automated feature extraction).

Alliances	Relative cover (%)	Number of polygons	Mean species richness	Standard deviation of species richness
*Pseudotsuga menziesii - Abies grandis**	28.1	26	21	4
*Alnus rubra - Umbellularia californica - Lithocarpus densiflorus**	24.7	19	16	4
*Lithocarpus densiflorus - Umbellularia californica - Pseudotsuga menziesii**	19.7	16	14	5
*Pseudotsuga menziesii - Umbellularia californica**	13.0	19	20	4
*Pseudotsuga menziesii**	6.9	14	19	6
Introduced perennial grassland*	3.6	6	13	2
Pine plantation*	1.0	2	21	4
Fraxinus latifolia	0.8	5	21	2
Acer macrophyllum	0.7	6	23	6
Salix sp.	0.7	4	22	11
Ceanothus thyrsiflorus	0.6	3	18	2
Baccharis pilularis	0.1	2	4	0
Quercus garryana	0.1	1	17	0

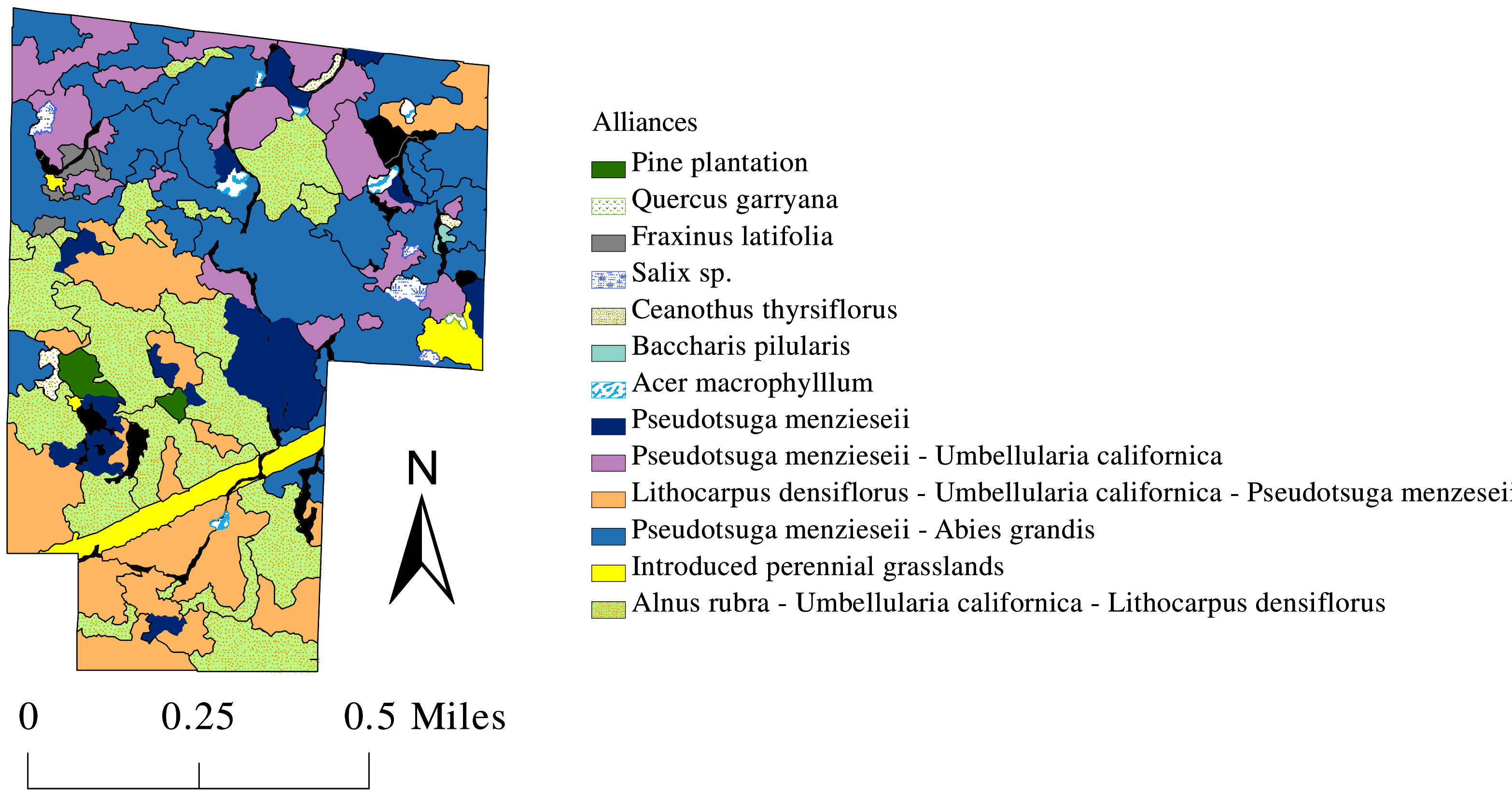

Figure 5. Thematic map showing seven vegetative alliances used in classification. Areas in black were masked as non-vegetation during analysis.

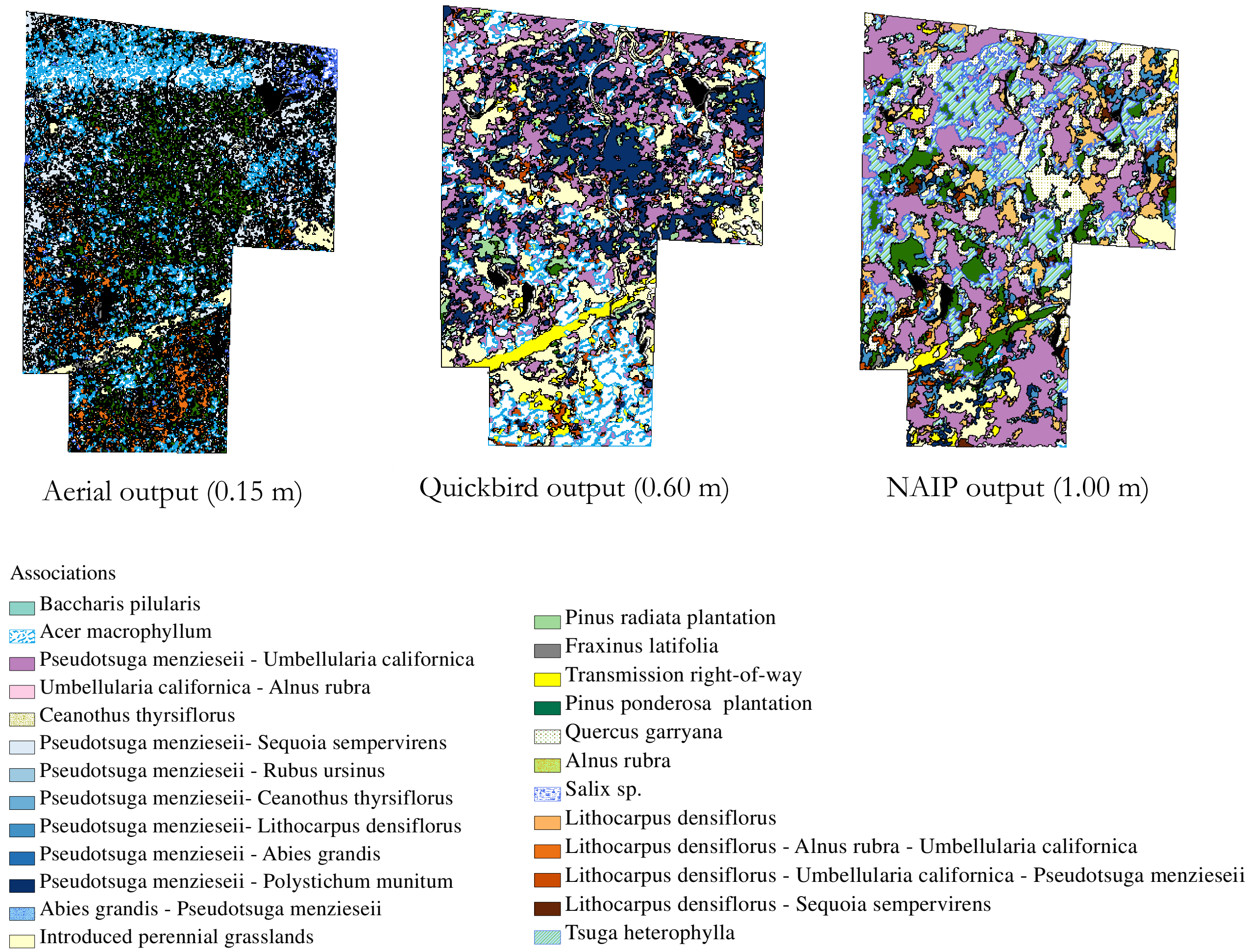

Figure 6. Feature analyst output association maps by image type. Areas in black were masked as non-vegetation during analysis.

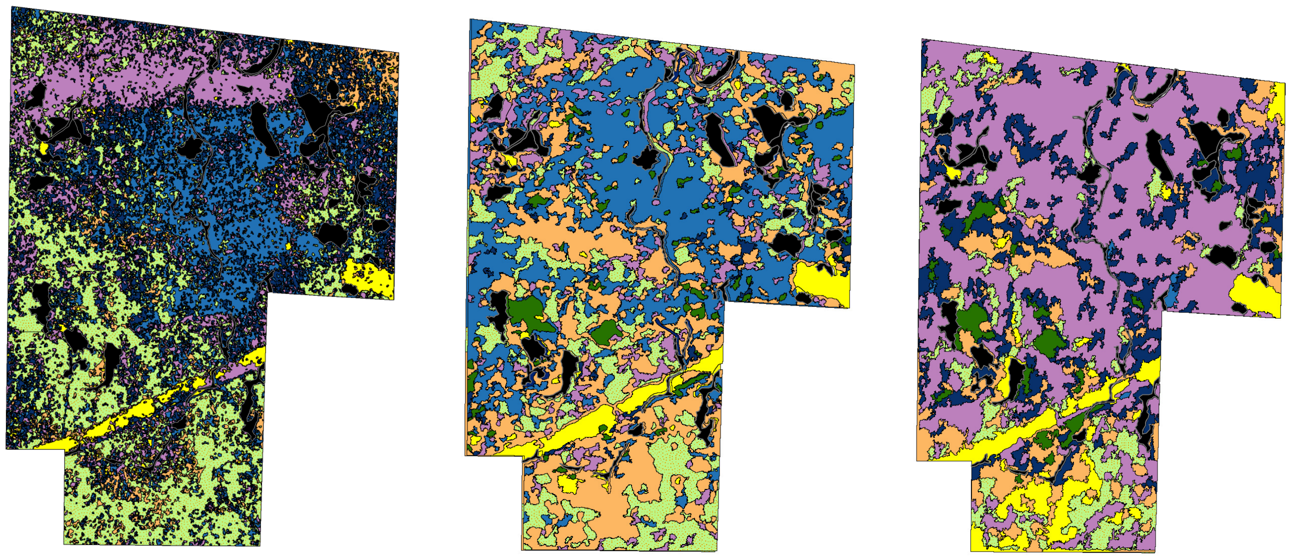

Aerial output (0.15 m) Quickbird output (0.60 m) NAIP output (1.00 m)

Alliances
- Pine plantation
- Pseudotsuga menzieseii
- Pseudotsuga menzieseii - Umbellularia californica
- Lithocarpus densiflorus - Umbellularia californica - Pseudotsuga menzeseii
- Pseudotsuga menzieseii - Abies grandis
- Introduced perennial grasslands
- Alnus rubra - Umbellularia californica - Lithocarpus densiflorus

Figure 7. Feature analyst output alliance maps by image type. 7 vegetative alliances used in classification are shown. Areas in black were masked as non-vegetation during analysis.

Table 4. Overall alliance output map accuracies by image type and analysis. Band numbers used in analysis in parentheses.

Image Spatial Resolution	All available bands a.	VNIR removed (3-band) b.	Select bands c.	NDVI d.
NAIP (1.00m)	0.37 (1,2,3)	n/a	0.41 (2,3)	n/a
Quickbird (0.60m)	0.69 (1,2,3,4)	0.60 (1,2,3)	0.47 (2,3)	0.54 (1,2,3,4,5)
Air photo (0.15 m)	0.48 (1,2,3,4)	0.27 (1,2,3)	0.33 (1,3,4)	0.37 (1,2,3,4,5)

The addition of the commonly used NDVI also did not improve overall accuracy (Table 4, column d). Overall accuracies decreased for the Quickbird and aerial images when resampled to 1m, implying a positive influence on accuracy from the VNIR band (Fig. 8). The highest overall accuracies for the Quickbird and aerial output maps were produced through the inclusion of all 4 bands and no further manipulation. The highest overall accuracy for the NAIP output map (41%) was produced through the removal of band 1.

The error matrices for each image (Table 5) reveal that the pine plantation and introduced perennial grassland classes generally had the highest user and producer accuracies. The pine plantations were misclassified, however, as *A. rubra* in the aerial output map. There was little consistency with other class accuracies or relative cover values (Table 6) across image types. The *A. rubra* dominant class had high user and producer accuracies but was confused with the *P. menziesii – Umbellularia californica*. The *P. menziesii – U. californica* and *P. menziesii – L. densiflorus* classes performed differently across images, however the *P. menziesii – L. densiflorus* class had relatively high user accuracies suggesting that, when identified, these classes were labeled appropriately. The *P. menziesii* class had the lowest producer accuracies (5-36%) and was frequently confused with the mixed *P. menziesii – A. grandis* class.

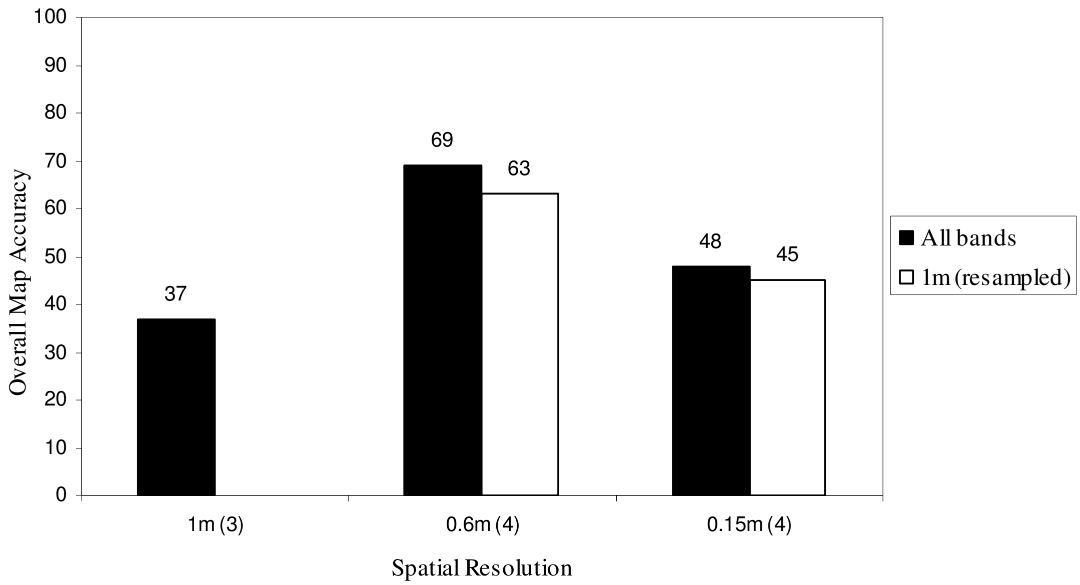

Figure 8. Overall accuracies of original and images resampled to 1 m. Number of spectral bands in parentheses.

Table 5. Error matrices for alliance map classification results by image type. Values represent area (m^2) classified. Vegetation classes for the L.W. Schatz study site include: (1) Alnus rubra - Umbellularia californica - Lithocarpus densiflorus (A-Uc-Ld); (2) Pseudotsuga menziesii (Pm); (3) Pseudotsuga menziesii - Umbellularia californica (P -Uc); (4) Pseudotsuga menziesii - Abies grandis (Pm-Ag); (5) Lithocarpus densiflorus - Umbellularia californica - Pseudotsuga menziesii (Ld-Uc-Pm); (6) Introduced perennial grasslands (IPG); and (7) Pine plantation (P).

Classified data	Reference data							
Class	A-Uc-Ld	Pm	Pm-Uc	Pm-Ag	Ld -UcPm	IPG	P	User (%)
(1) Classification error matrix for the aerial photo (0.15 m, 4-band)								
A-Uc-Ld	294645	21856	66020	49650	182548	0	11126	47
Pm	0	4511	0	30454	0	0	0	13
Pm-Uc	6606	12884	74008	145180	0	0	0	31
Pm-Ag	43939	59141	37805	192590	52480	0	3750	49
Ld-Uc-Pm	0	0	0	2	43069	0	0	100
IPG	0	0	0	0	0	54014	0	100
P	0	0	0	0	0	0	0	0
Producer (%)	85	5	42	46	15	100	0	
Overall (%)								48
K_{hat}								0.33
(2) Classification error matrix for the Quickbird image (0.60 m, 4-band)								
A-Uc-Ld	248618	0	47270	2	0	0	0	82
Pm	0	5707	0	0	0	0	0	100
Pm-Uc	0	0	12261	14645	0	0	0	46
Pm-Ag	68084	29170	68856	348958	0	595	0	69
Ld-Uc-Pm	28489	61969	49446	54271	278098	0	0	59
IPG	0	0	0	0	0	53419	0	100
P	0	1545	0	0	0	0	14876	90
Producer (%)	70	6	7	85	100	99	100	
Overall (%)								69
K_{hat}								0.43
(3) Classification error matrix for the NAIP image (1.0 m, 3-band)								
A-Uc-Ld	68111	3821	0	0	0	0	0	95
Pm	658	35886	3777	48625	15961	0	0	34
Pm-Uc	275181	50215	174056	369251	40984	0	0	19
Pm-Ag	0	0	0	0	0	0	0	
Ld-Uc-Pm	0	6927	0	0	173858	982	0	96
IPG	1240	0	0	0	47295	52429	0	52
P	0	1544	0	0	0	603	14876	87
Producer (%)	20	36	98	0	63	97	100	
Overall (%)								37
K_{hat}								0.28

Table 6. Relative cover values of alliances for Feature Analyst output maps by image type.

Alliance	Aerial image	Quickbird image	NAIP image	Reference map
Pseudotsuga menziesii - Abies grandis	24.0	33.1	0.3	28.1
Alnus rubra - Umbellularia californica - Lithocarpus densiflorus	30.4	17.1	9.0	23.7
Lithocarpus densiflorus - Umbellularia californica - Pseudotsuga menziesii	6.9	31.0	11.8	18.7
Pseudotsuga menziesii - Umbellularia californica	20.8	9.4	50.8	12
Pseudotsuga menziesii	14.5	1.8	16.9	6.6
Introduced perennial grassland	3.3	4.3	8.1	3.6
Pine plantation	0.2	3.3	3.2	1

When the *P. menziesii* and *P. menziesii – A. grandis* classes were combined into a "mixed conifer" class the overall accuracies of the air photo, Quickbird, and NAIP images increased to 54%, 72%, 41%, respectively.

Differences in vegetation class accuracies were evaluated using a non-parametric Kruskal-Wallis ANOVA procedure, followed by Kruskal-Wallis Z and Bonferroni correction. Significant differences ($p < 0.05$) between the accuracies of vegetation types for each image were detected (Figure 9).

3.1. Sources of Error

Spectral separation of classes was calculated for all three images using the transformed divergence statistic (Swain and Davis, 1978; ERDAS IMAGINE, 2005). Results showed that all images did not have ideal spectral separation implying spectral overlap between classes. The Quickbird data had the best statistical separation between categories. All images had similar minimum values. In general, the classes with the highest producer and user accuracies had the highest spectral separation (Appendix B). The introduced perennial grass class was the most spectrally distinct with the highest transform divergence values across all images (air photo = 995, Quickbird = 1432, NAIP = 503 average TD). Classes that were confused with each other typically had transformed divergence values <100 but were not always those with the highest spectral overlap. For example, in the aerial image the pine plantation class was confused with the *Alnus rubra - Umbellularia californica - Lithocarpus densiflorus* class (TD = 227) and not the *Pseudotsuga menziesii* class (TD = 17).

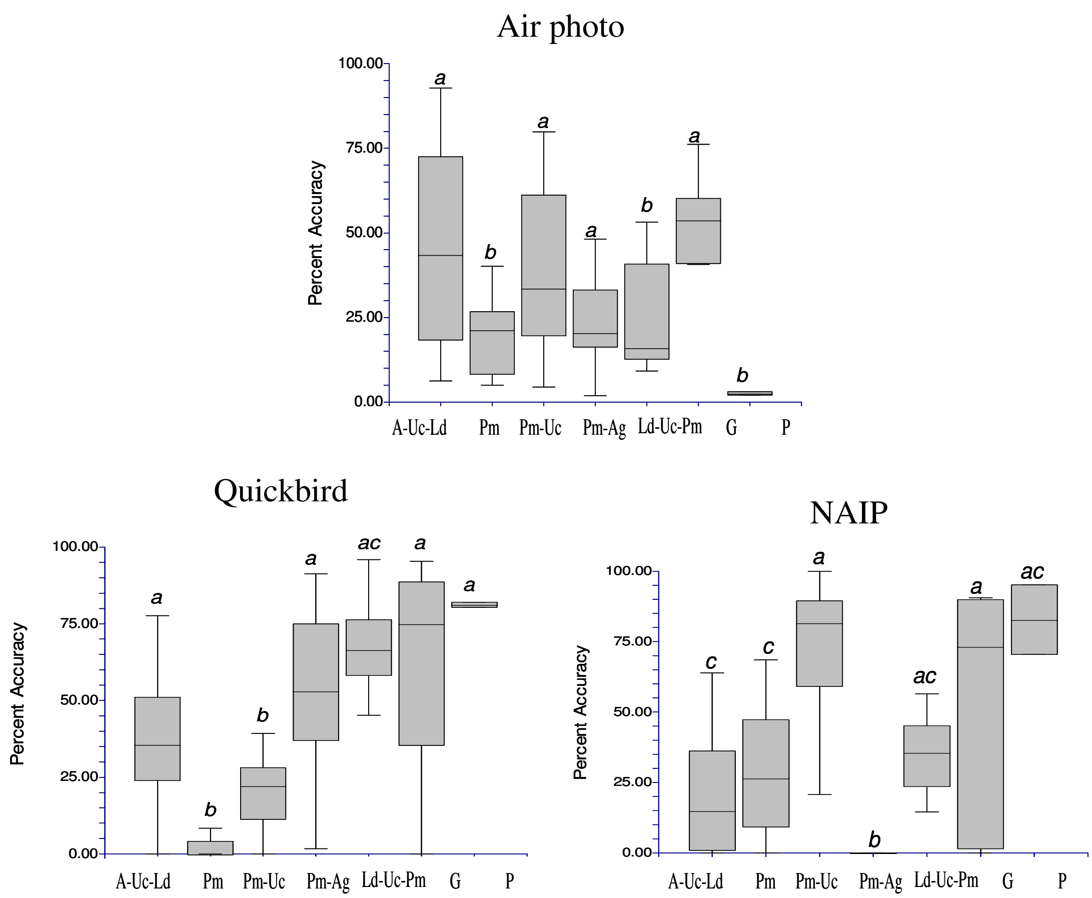

Figure 9. ANOVA test for differences in vegetation class accuracy across image types. Different letters above the bars indicate significant differences in Tukey post-hoc comparisons between the classes. Vegetation codes are defined in Table 5.

Increasing internal variability in vegetation classes is correlated with decreasing classification accuracy (Cushnie, 1987; Cochrane, 2000). Higher intra-class variability lessens the separation between classes, making thematic distinction difficult. The average standard deviations of the digital numbers within vegetation types revealed differences across images. The air photo has the most intra-class variability (31.1) which may be due to the high number of pixels. It did not, however, have the lowest accuracies when all 4 bands were used, implying an important contribution from the VNIR band. The Quickbird image had the least amount of intra-class variance (11.2) and the highest accuracies.

Although factors such as polygon size, total vegetation coverage, and number of training polygons have been shown to influence accuracy (Foody et al., 1995; Foody and Arora, 1997; Staufer and Fischer, 1997; Ellis and Wang, 2006; Foody and Mathur, 2006), logistic and linear regressions of these variables did not result in significant findings with the exception of the NAIP image where producer accuracy increased as class coverage decreased ($p = 0.03$). This relationship is exemplified in the pine plantation high accuracies despite low cover (1%) and low number of training polygons (2).

4. Discussion

In all cases, the Quickbird image produced the highest levels of overall accuracy when compared to the air photo and the NAIP image. Image processing techniques, such as resampling, inclusion of an NDVI, selection of bands with the highest transformed divergence values, or use of natural color bands (R, G, B) alone, did not alter this outcome. These techniques did, however, generally lower the overall and class accuracies of the Quickbird and air photo. The highest overall accuracies for these two images were produced using all available bands. The highest accuracy for the NAIP image, however, resulted from the removal of the blue band (450 – 520 nm). Blue bands can add unwanted noise to an image oftentimes due to atmospheric scattering (Kimes et al., 2006). The NDVI did not produce higher accuracies since this index generally compensates for terrain effects such as surface slope, aspect, or elevation, (Lillesand et al., 2004) and these factors were not significantly different between vegetation types. Additionally, the addition of the NDVI may have also added unwanted noise through the inclusion of redundant reflectance values.

What accounts for these differences in image performance? Generally speaking it results from the software's ability to discriminate between classes. Spectral separation and internal variability of classes were predominant factors influencing class discernment (Cushnie, 1987; Cochrane, 2000). An increase in intra-class variability causes a reduction of statistical separability between classes (Cushnie, 1987; Yu et al., 2006).

The Quickbird image had the highest overall transformed divergence values, the lowest intra-class variability, and the highest accuracies. This pattern was also found with the pine plantation and introduced perennial grass vegetation types. High accuracies occurred in these classes despite their low percentage of vegetative cover, as well as small number of training polygons (Foody, 2002; Chubey et al., 2006) suggesting that spectral separation supersedes these other variables in effect.

Another mechanism behind image performance relates to spatial resolution. It can be difficult to assess the appropriate threshold for spatial resolution. Too fine a resolution may increase the internal variability within homogeneous land cover units too much (Woodcock and Strahler, 1987; Aplin et al., 1997; Greenberg et al., 2006; Yu et al., 2006). At too coarse a resolution a number of vegetation types may be combined within one pixel, resulting in a spectrally noisy signal and yielding poor classification results (Cushnie, 1987; Yu et al., 2006; Johansen et al., 2007). The results of the 3-band input trials imply that a 0.6 m spatial scale may be best suited for alliance-level classification, followed by 1 m and finally 0.15 m. The higher resolution aerial photo may aid in visual interpretation, but it is not a 'best fit' when using automated classifiers.

Accuracies less than 80% may be due to land management history and to the early seral stages in this landscape (Jiang et al., 2004; Lu, 2005; Rapp et al., 2005). My study site was a heterogeneous mosaic of young forest, plantation, and remnant old-growth trees typical of post-logged coniferous forests in the Pacific Northwest today (Spies et al., 1994; Jiang et al., 2004). Due to fragmentation of the landscape and resultant growth patterns, vegetation classes were rarely composed of solely one or two dominant species, such as a pine or grass, but were instead a mix of conifer and hardwood species of varying ages and sizes. For example, some classes defined by the Federal Geographic Data Committee (1997) have differences of 10% tree cover in some of their alliances which would not consistently produce a significant change in spectral signal (Greenberg et al., 2006). Dissimilarities in structural attributes of forest stands may have a greater effect on reflectance characteristics than tree species composition (Lefsky and Cohen, 2003). Additionally, evergreen forest types have been shown to lack unique spectral reflectance characteristics due to limited phenological differences (Lillesand et al., 2004). In my study the most ecologically mixed classes tended to be the most confused. Although some interpreters emphasize the importance of spectrally 'pure' classes, there may be more inherent variability within one tree crown than between species or classes (Leckie et al., 1992). Thus, prioritizing class homogeneity may produce ecologically meaningless polygons.

Categorical scale is another important factor in classification (Marceau et al., 1994; Ju and Gopal, 2005; Rapp et al., 2005). The map of associations had extremely low accuracies likely due to large number of input classes and the presence of subcanopy vegetation (Greenberg et al., 2006). To date, LIDAR data has been most effective in directly measuring three-dimensional distributions of plant canopy and sub-canopy (Lefsky and Cohen, 2003) thus a laser-altimetry tool may be more suited for this level of detail. Other studies (Greenberg et al., 2006; Yu et al., 2006) have generally shown low accuracies when attempting to classify alliances because of the influence of sub-canopy vegetation, small sample sizes, and species co-dominance.

Additional issues affecting accuracy not directly explored in my study include positional error of GPS and imagery (Foody, 2002), temporal differences in image acquisition (Lefsky and Cohen, 2003), join lines in mosaicked aerial photos (Lefsky and Cohen, 2003), as well as accuracy assessment method (Gopal and Woodcock, 1994; Stehman, 1997; Foody, 2002; Liu et al., 2007).

Overall accuracies were somewhat low with fine scale classifications, and only one image approached the commonly used 80% accuracy threshold (Environmental Systems Research Institute and The Nature Conservancy, 1994). The software produced the highest accuracies when utilizing all available bands, thus removing the need for image enhancement or other interpreter-based processing techniques (Hay et al., 2005).

The specific algorithms employed by Feature Analyst software included a type of neural network classifier that considers spatial context, or image 'texture', in addition to the brightness values of the pixels (Visual Learning Systems, 2006). Neural network classifiers have been successful in supervised classification of community data owing in part to their non-parametric nature which is appropriate for non-normally distributed data (Černá and Chytrý, 2005), as well as their ability to learn by example and generalize (Foody and Arora, 1997). Although artificial neural networks have given accurate class predictions compared to other supervised methods they are also accused of having a 'black-box' approach (Černá and Chytrý, 2005) which hides the underlying process. Foody and Arora (1997) found that neural network classifiers performed well on small training sets, however this software could not resolve classes in the alliance map that were represented by only 1 polygon, regardless of size. Therefore, types that are 'rarer' such as *Tsuga heterophylla*, could not be identified through this process, and, it can be difficult to have enough polygons for training on such a small scale.

Additionally, the input representation pattern employed was limited in pixel number (100 per band). Therefore, less area was covered with each pass in the higher resolution images. This resulted in certain features of distinct shape, such as the electrical right-of-way, being misclassified in the association map. Thus, processing time would be extended by the necessity of running several passes or employing different input patterns to extract various shapes.

5. Conclusions

Object-oriented software may not be the ideal method to achieve high accuracy for alliance-level classification and mapping. Automated feature extraction has been shown to perform better in more homogeneous landscapes or at coarser categorical scales. To date, remote sensing is not as accurate and precise in measuring vegetation that an investigator utilizing manual and field-based mapping techniques can achieve (Greenberg et al., 2006). Thus, choosing this method of classification should be weighed against considerations such as cost and time limitations.

Spatial and spectral resolutions are important parameters to consider when choosing imagery for vegetation mapping. It is wise to use imagery at a spatial resolution that is appropriate for both the features being classified (Woodcock and Strahler, 1987) and the method of classification. In short, higher spatial resolution does not always produce the highest map accuracies with automated methods, and lower spatial resolution is not ideal for manual mapping. Additionally, the processing time associated with each image type should be considered as larger file sizes may lead to cumbersome hardware demands.

More work is needed to explore the utility of very high spatial resolution imagery in the field of vegetation classification and mapping. As satellites continue to offer finer pixel grains and additional spectral bands, they are fast becoming a viable choice over aerial imagery which is frequently cost-intensive. Additionally, more studies classifying second-growth heterogeneous vegetation to fine categorical scales are needed to adequately assess the application of object-oriented classification procedures on sites reflecting the changing landscape.

References

Aalto, K.R., Harper, G.D., 1989. Geologic evolution of the northernmost coast ranges and western Klamath mountains, California. American Geophysical Union, Washington, DC.

Anderson, K.R., Harper, G.D., Roach, J.T., Witmer, R.E., 1976. A land use and land cover classification system for use with remote sensor data. USGS Survey, Government Printing Office, Washington, DC.

Aplin, P., Atkinkson, P.M., Curran, P.J., 1997. Fine spatial resolution satellite sensors for the next decade. Int. J. of Remote Sens. 18, 3873-3881.

Asner, P.G., Hicke, J.A., Lobell, D.B., 2003. Per-pixel analysis of forest structure: Vegetation indices, spectral mixture analysis and canopy reflectance modeling. In: Wulder, M.A., Franklin, S.E. (Eds.), Remote Sensing of Forest Environments: Concepts and Case Studies. Kluwer Academic Publishers, Norwell, Massachusetts, pp. 13-46.

Barbarella, M., Lenzi, V., Zanni, M., 2004. Integration of airborne laser data and high resolution satellite images over landslides risk areas. Int. Arch. .Photogramm. Remote Sens. Spatial Info. Sci. 35, 945-950.

Benson, B.J., MacKenzie, M.D., 1995. Effects of sensor spatial resolution on landscape structure parameters. Lands. Ecol. 10, 113-120.

Braun-Blanquet, J., 1932. Plant sociology. McGraw-Hill, New York, New York.

California Native Plant Society, 2004. California Native Plant Society relevé protocol. California Native Plant Society, Sacramento, California.

Carleer, A., Wolff, E., 2004. Exploitation of very high resolution satellite data for tree species identification. Photogramm. Eng. Remote Sens. 70, 135-140.

Černá, L., Chytrý, M., 2005. Supervised classification of plant communities with artificial neural networks. J. Veg. Sci. 16, 407-414.

Chubey, M.S., Franklin, S.E., Wulder, M.A., 2006. Object-based analysis of Ikonos-2 imagery for extraction of forest inventory parameters. Photogramm. Eng. Remote Sens. 72, 383-394.

Cochrane, M.A., 2000. Using vegetation reflectance variability for species level classification of hyperspectral data. Int. J. of Remote Sens. 21, 2075-2087.

Colwell, W., DeLapp, J., Gladish, E., 1960. California Cooperative Soil Vegetation Survey, Humboldt County. In, Soil - Vegetation Map Series. Pacific Southwest Forest & Range Experimental Station (USFS).

Congalton, R.G., Green, K., 1999. Assessing the accuracy of remotely sensed data: principles and practices. Lewis Publications, Boca Raton.

Cooper, A., McCann, T., Bunce, R.G.H., 2006. The influence of sampling intensity on vegetation classification and the implications for environmental management. Environ. Cons. 33, 118-127.

Cushnie, J.L., 1987. The interactive effect of spatial resolution and degree of internal variability within land-cover types on classification accuracies. Int. J. of Remote Sens. 8, 15-29.

Ellis, E.C., Wang, H., 2006. Estimating area errors for fine-scale feature-based ecological mapping. Int. J. of Remote Sens. 27, 4731-4749.

Environmental Systems Research Institute, 2006. ArcGIS 9: Using ArcGIS Desktop. ESRI Press, Redlands, California.

Environmental Systems Research Institute and The Nature Conservancy, 1994. USGS-NPS vegetation mapping program: field methods for vegetation mapping. United States Department of the Interiro, Washington, D.C.

ERDAS IMAGINE, 2005. Erdas Imagine Field Guide. ERDAS Inc., Atlanta, Georgia.

Federal Geographic Data Committee, 1997. Vegetation Classification Standard: FGDC-STD-005, U.S. Geological Survey, Reston, Virginia.

Foody, G.M., 2002. Status of land cover classification accuracy assessment. Remote Sens. Environ. 8, 185-201.

Foody, G.M., Arora, M.K., 1997. An evaluation of some factors affecting the accuracy of classification by an artificial neural network. Int. J. of Remote Sens. 18, 799-810.

Foody, G.M., Mathur, A., 2006. The use of small training sets containing mixed pixels for accurate hard image classification: Training on mixed spectral responses for classification by a SVM. Remote Sens. Environ. 103, 179-189.

Foody, G.M., McCulloch, M.B., Yates, W.B., 1995. Classification of remotely sensed data by an artificial neural network: issues related to training data characteristics. Photogramm. Eng. Remote Sens. 61, 391-401.

Gopal, S., Woodcock, C.E., 1994. Theory and methods for accuracy assessment of thematic maps using fuzzy sets. Photogramm. Eng. Remote Sens. 60, 181-188.

Greenberg, J.A., Dobrowski, S.Z., Ramirez, C.M., Tull, J.L., Ustin, S.L., 2006. A bottom-up approach to vegetation mapping of the Lake Tahoe Basin using hyperspatial image analysis. Photogramm. Eng. Remote Sens. 72, 581-589.

Hall, R.J., 2003. The roles of aerial photographs in forestry remote sensing image analysis. In: Wulder, M.A., Franklin, S.E. (Eds.), Remote Sensing of Forest Environments: Concepts and Case Studies. Kluwer Academic Publishers, Norwell, Massachusetts, pp. 47-76.

Halpern, C.B., Spies, T.A., 1995. Plant species diversity in natural and managed forests of the Pacific Northwest. Ecol. Appl. 5, 913-934.

Hay, G.J., Castilla, G., Wulder, M.A., Ruiz, J.R., 2005. An automated object-based approach for the multiscale image segmentation of forest scenes. J. Appl. Earth Obs. Geoinfo. 7, 339-359.

Jensen, J.R., 2000. Remote Sensing of the Environment: An Earth Resource Perspective. Prentice Hall, Upper Saddle River, New Jersey.

Jiang, H., Strittholt, J.R., Frost, P.A., Slosser, N.C., 2004. The classification of late seral forests in the Pacific Northwest, USA using Landsat ETM+ imager. Remote Sens. Environ. 91, 320-331.

Johansen, K., Coops, N.C., Gergel, S.E., Strange, Y., 2007. Application of high spatial resolution satellite imagery for riparian and forest ecosystem classification. Remote Sens. Environ.110, 29-44.

Ju, J., Gopal, S., 2005. On the choice of spatial and categorical scale in remote sensing land cover classification. Remote Sens. Environ. 96, 62-77.

Kimes, D.S., Ranson, K.J., Sun, G., Blair, J.B., 2006. Predicting LIDAR measured forest vertical structure from multi-angle spectra data. Remote Sens. Environ. 100, 503-511.

Leckie, D.G., Gourgeon, F.A., Tinis, S., Nelson, T., Burnett, D., Paradine, D., 2005. Automated tree recognition in old growth conifer stands with high resolution digital imagery. Remote Sens. Environ. 94, 311-326.

Leckie, D.G., Yuan, X., Ostaff, D.P., Piene, H., MacLean, D.A., 1992. Analysis of high resolution multispectral MEIS imagery for spruce budworm damage assessment on a single tree basis. Remote Sens. Environ. 40, 125-136.

Lee, C., 2004. Vegetation alliances and associations of the Whiskeytown National Recreation Area. Master's thesis. Department of Forestry & Watershed Management. Humboldt State University, Arcata, California.

Lefsky, A.M., Cohen, W.B., 2003. Selection of Remotely Sensed Data. In: Wulder, M.A., Franklin, S.E. (Eds.), Remote Sensing of Forest Environments: Concepts and Case Studies. Kluwer Academic Publishers, Norwell, Massachusetts, pp. 13-46.

Lillesand, T.M., Kieffer, R.W., Chipman, J.W., 2004. Remote Sensing and Image Interpretation, 5th edition. John Wiley & Sons Inc., New York, New York.

Liu, C., Frazier, P., Kumar, L., 2007. Comparative assessment of the measures of thematic classification accuracy. Remote Sens. Environ. 107, 606-616.

Lu, D., 2005. Integration of vegetation inventory data and Landsat TM image for vegetation classification in the western Brazilian Amazon. For. Ecol. Manage. 213, 369-383.

Marceau, D.J., Howarth, P.J., Gratto, D.J., 1994. Remote Sensing and the measurement of geographical entities in a forested environment. The scale and spatial aggregation problem. Remote Sens. Environ. 49, 93-104.

McCune, B., Grace, J.B., 2002. Analysis of ecological communities. MjM Software, Gleneden Beach, Oregon.

Mueller-Dombois, D., Ellenberg, H., 1974. Aims and Methods of Vegetation Ecology. John Wiley & Sons, Inc., New York, New York.

Mullerova, J., 2004. Use of digital aerial photography for sub-alpine vegetation mapping: A case study from the Krkonose Mts., Czech Republic. Plant Ecology 175, 259-272.

Rapp, J., Wang, D., Capen, D., Thompson, E., Lautzenheiser, T., 2005. Evaluating error in using the national vegetation classification system for ecological community mapping in Northern New England, USA. Natural Areas Journal 25, 46-54.

Ripley, B.D., 1996. Pattern Recognition and Neural Networks. Cambridge University Press, London, England.

Rosenfield, G.H., Fitzpatrick-Lins, K., 1986. A coefficient of agreement as a measure of thematic classification accuracy. Photogramm. Eng. Remote Sens. 52, 223-227.

Sandmann, H., Lertzman, K.P., 2003. Combining high-resolution aerial photography with gradient-directed transects to guide field sampling and forest mapping in mountainous terrain. For. Sci. 49, 429-443.

Sawyer, J.O., Keeler-Wolf, T., 1995. Manual of California Vegetation. California Native Plant Society Press, Sacramento, California.

Schatz, G., 2007. Personal Communication. 14345 Maple Creek Route, Korbel, CA 95550.

Song, M., Civco, D.L., Hurd, J.D., 2005. A competitive pixel-object approach for land cover classification. Int. J. of Remote Sens. 26, 4981-4997.

Spies, T.A., Ripple, W.J., Bradshaw, G.A., 1994. Dynamics and pattern of a managed coniferous forest landscape. Ecological Applications 4, 555-568.

Staufer, P., Fischer, M.M., 1997. Spectral pattern recognition by a two layer perceptron: Effects of training set size. In: Kanellopoulos, I., Wilkinson, G., Roli, F., Austin, J. (Eds.), Neurocomputation in Remote Sensing Data Analysis. Springer-Verlag, Berlin, Germany, pp. 105-116.

Stehman, S.V., 1997. Selecting and interpreting measures of thematic classification accuracy. Remote Sens. Environ. 62, 77-89.

Stohlgren, T.J., Chong, G.W., Kalkhan, M.A., Schell, L.D., 1997. Multiscale sampling of plant diversity: Effects of minimum mapping unit size. Ecol. Appl. 7, 1064-1074.

Story, M., Congalton, R.G., 1986. Accuracy assessment: A user's perspective. Photogramm. Eng. Remote Sens. 52, 397-399.

Swain, M., Davis, S.M., 1978. Remote Sensing: The Quantitative Approach. McGraw-Hill Inc., New York, New York.

USDA, 2002. Existing Vegetation Classification and Mapping Technical Guide (Draft). USDA Forest Service, Washington, D.C.

USDA, 2007. The PLANTS Database (http://plants.usda.gov, 19 October 2007). National Plant Data Center, Natural Resources Conservation Service, Baton Rouge, Louisiana.

Vanderzanden, D., Morrison, M., 2003. High Resolution Image Classification: A Forest Service Test of Visual Learning System's Feature Analyst. USDA Forest Service, Salt Lake City, Utah.

Visual Learning Systems, 2006. Feature Analyst Version 4.1 for Arc GIS Reference Manual. Visual Learning Systems Inc., Missoula, Montana.

Woodcock, C.E., Strahler, A.H., 1987. The factor of scale in remote sensing. Remote Sens. Environ. 21, 311-332.

Wulder, M.A., Hall, R.J., Coops, N.C., Franklin, S.E., 2004. High spatial resolution remotely-sensed data for the study of forest ecosystems. Bioscience 54, 511-521.

Yildirim, A., Seker, D.Z., 2004. Country-based analysis of the investment dimension of the airborne and spaceborne imagery. In, Proceedings of XXth ISPRS Congress, 12-23 July 2004, Istanbul, Turkey.

Yu, Q., Gong, P., Clinton, N., Biging, G., Kelly, M., Schirokauer, D., 2006. Object-based detailed vegetation classification with airborne high spatial resolution remote sensing imagery. Photogramm. Eng. Remote Sens. 72, 799-811.

Appendix A. Vascular plant species found in study location. Nomenclature follows the USDA PLANTS Database (USDA, 2007).

Family	Species	Common name
Aceraceae	*Acer macrophyllum* Pursh	bigleaf maple
Aceraceae	*Acer circinatum* Pursh	vine maple
Anacardiaceae	*Toxicodendron diversilobum* (Torr. & Gray) Greene	Pacific poison-oak
Apiaceae	*Daucus carota* L.	wild carrot
Apiaceae	*Heracleum maximum* Bartr.	cow parsnip
Apiaceae	*Osmorhiza chilensis* Hook. & Arn.	mountain sweet cicely
Apiaceae	*Sanicula crassicaulis* Poepp. ex DC.	Pacific blacksnakeroot
Araliaceae	*Aralia californica* S. Wats.	elk clover
Aristolochiaceae	*Asarum caudatum* Lindl.	wild ginger
Asteraceae	*Achillea millefolium* L.	common yarrow
Asteraceae	*Adenocaulon bicolor* Hook.	American trailplant
Asteraceae	*Baccharis pilularis* DC.	coyotebrush
Asteraceae	*Cirsium vulgare* (Savi) Ten.	bull thistle
Asteraceae	*Erechtites minima* (Poir.) DC.	coastal burnweed
Asteraceae	*Gnaphalium* sp. L.	cudweed
Asteraceae	*Hieracium albiflorum* Hook.	white hawkweed
Asteraceae	*Leucanthemum vulgare* Lam.	oxeye daisy
Asteraceae	*Madia elegans* D. Don ex Lindl.	common madia
Asteraceae	*Petasites palmatus* (Ait.) Gray	coltsfoot
Asteraceae	*Taraxacum officinale* G.H. Weber ex Wiggers	dandelion
Berberidaceae	*Achlys californica* Fukuda & Baker	California deer-foot
Berberidaceae	*Mahonia repens* (Lindl.) G. Don	Oregon grape
Berberidaceae	*Vancouveria hexandra* (Hook.) Morr. & Dcne.	white insideout flower
Betulaceae	*Alnus rubra* Bong.	red alder
Betulaceae	*Corylus cornuta* var. *californica* (A. DC.) Sharp	California hazelnut
Blechnaceae	*Blechnum spicant* (L.) Sm.	deer fern
Boraginaceae	*Plagiobothrys* sp. Fisch. & C.A. Mey.	popcorn flower
Caprifoliaceae	*Lonicera hispidula* (Lindl.) Dougl. ex Torr. & Gray	honeysuckle
Caprifoliaceae	*Sambucus racemosa* L.	red elderberry
Caprifoliaceae	*Symphoricarpos albus* (L.) Blake	common snowberry
Caryophyllaceae	*Stellaria media* (L.) Vill.	common chickweed
Celastraceae	*Euonymus occidentale* Nutt. ex Torr. var. *occidentale*	western burning bush
Clusiaceae	*Hypericum perforatum* L.	common St. Johnswort
Cornaceae	*Cornus sericea* L.	American dogwood
Cucurbitaceae	*Marah oreganus* (Torr. ex S. Wats.) T.J. Howell	coastal manroot
Cupressaceae	*Sequoia sempervirens* (Lamb. ex D. Don) Endl.	coast redwood
Cupressaceae	*Sequoiadendron giganteum* (Lindl.) Buchh.	giant sequoia
Cyperaceae	*Carex deweyana* Schwein.	Dewey's sedge
Cyperaceae	*Carex obnupta* Bailey	slough sedge
Cyperaceae	*Carex* sp. L.	sedge
Cyperaceae	*Cyperus eragrostis* Lam.	tall flatsedge
Dennstaedtiaceae	*Pteridium aquilinum* (L.) Kuhn	bracken fern

Appendix A. Vascular plant species found in study location. Nomenclature follows yhe USDA PLANTS Database (USDA, 2007; continued).

Family	Species	Common name
Dipsacaceae	*Dipsacus fullonum* L.	Fuller's teasel
Dryopteridaceae	*Athyrium filix-femina* (L.) Roth	lady fern
Dryopteridaceae	*Polystichum munitum* (Kaulfuss)	sword fern
Equisetaceae	*Equisetum arvense* L.	common horsetail
Equisetaceae	*Equisetum hyemale* L. var. *affine* (Engelm.) A.A. Eat.	giant scouring rush
Ericaceae	*Arbutus menziesii* Pursh	Pacific madrone
Ericaceae	*Arctostaphylos columbiana* Piper	hairy manzanita
Ericaceae	*Gaultheria shallon* Pursh	salal
Ericaceae	*Vaccinium ovatum* Pursh	evergreen huckleberry
Ericaceae	*Vaccinium parvifolium* Sm.	red huckleberry
Fabaceae	*Lathyrus sp.* L.	sweet-pea
Fabaceae	*Lotus corniculatus* L.	broadleaf birdsfoot trefoil,
Fabaceae	*Lupinus sp.* L.	lupine
Fabaceae	*Melilotus alba* (L.) Lam.	yellow sweetclover
Fabaceae	*Trifolium sp.* L.	clover
Fabaceae	*Vicia sativa* L.	spring vetch
Fagaceae	*Chrysolepis sempervirens* Kellogg Hjelmqvist	bush chinquapin
Fagaceae	*Lithocarpus densiflorus* (Hook. & Arn.) Rehd.	tanoak
Fagaceae	*Quercus garryana* Dougl. ex Hook.	Oregon white oak
Gentianaceae	*Centaurium muehlenbergii* (Griseb.) W. Wight ex Piper	Muhlenberg's centaury
Geraniaceae	*Geranium dissectum* L.	cut-leaved geranium
Grossulariaceae	*Ribes bracteosum* Dougl. ex Hook.	stink currant
Grossulariaceae	*Ribes menziesii* Pursh	canyon gooseberry
Grossulariaceae	*Ribes sanguineum* Pursh	red-flowering currant
Hydrangeaceae	*Whipplea modesta* Torr.	yerba de selva
Hydrophyllaceae	*Hydrophyllum tenuipes* Heller	Pacific waterleaf
Hydrophyllaceae	*Nemophila pedunculata* Dougl. ex Benth.	littlefoot nemophila
Hydrophyllaceae	*Phacelia* sp. Juss	phacelia
Iridaceae	*Iris douglasiana* Herbert	Douglas iris
Iridaceae	*Sisyrinchium bellum* S. Wats.	blue-eyed-grass
Juncaceae	*Juncus patens* E. Mey.	spreading rush
Juncaceae	*Juncus sp.* L.	rush
Lamiaceae	*Mentha arvensis* L.	wild mint
Lamiaceae	*Prunella vulgaris* L.	self heal
Lamiaceae	*Satureja douglasii* (Benth.) Kuntze	yerba buena
Lamiaceae	*Stachys rigida* Nutt. ex Benth. var. *rigida*	rigid hedge-nettle
Lauraceae	*Umbellularia californica* (Hook. & Arn.) Nutt.	California bay
Liliaceae	*Chlorogalum* sp. Kunth	soap plant
Liliaceae	*Clintonia andrewsiana* Torr.	bead lily
Liliaceae	*Dichelostemma capitatum* (Benth.) Wood	bluedicks
Liliaceae	*Dichelostemma ida-maia* (Wood) Greene	firecracker flower
Liliaceae	*Disporum hookeri* Torr.	Hooker's fairy bells
Liliaceae	*Lilium kelloggii* Purdy	Kellog's Lily
Liliaceae	*Lilium* sp. L.	lily
Liliaceae	*Scoliopus bigelovii* Torr.	fetid adder's tongue

Appendix A. Vascular plant species found in study location. Nomenclature follows the USDA PLANTS Database (USDA, 2007; continued).

Family	Species	Common name
Liliaceae	*Maianthemum racemossum* (L.) Link	false lily of the valley
Liliaceae	*Maianthemum stellatum* (L.) Link	starry false lily of the valley
Liliaceae	*Trillium ovatum* Pursh	coast trillium
Linaceae	*Linum bienne* P. Mill.	pale flax
Oleaceae	*Fraxinus latifolia* Benth.	Oregon ash
Onagraceae	*Circaea alpina* L.	enchanter's nightshade
Onagraceae	*Epilobium* sp. L.	fireweed
Orchidaceae	*Corallorrhiza striata* Lindl.	striped coral root
Oxalidaceae	*Oxalis oregana* Nutt.	redwood sorrel
Papaveraceae	*Dicentra formosa* (Haw.) Walp.	Pacific bleeding heart
Philadelphaceae	*Philadelphus lewisii* Pursh ssp. *californicus* (Benth.) Munz	wild mock orange
Pinaceae	*Abies grandis* (Dougl. ex D. Don) Lindl.	grand fir
Pinaceae	*Pinus ponderosa* P.& C. Lawson	ponderosa pine
Pinaceae	*Pinus radiata* D. Don	Monterey pine
Pinaceae	*Pinus sylvestris* L.	Scot's pine
Pinaceae	*Pseudotsuga menziesii* (Mirbel) Franco	Douglas-fir
Pinaceae	*Tsuga heterophylla* (Raf.) Sarg.	western hemlock
Plantaginaceae	*Plantago lanceolata* L.	narrow-leaved plantain
Poaceae	*Agrostis stolonifera* L.	creeping bentgrass
Poaceae	*Anthoxanthum odoratum* L.	sweet vernal grass
Poaceae	*Avena* sp. L.	oats
Poaceae	*Briza minor* L.	little rattlesnake grass
Poaceae	*Bromus hordeaceus* L.	soft brome
Poaceae	*Cortaderia jubata* (Lem.) Stapf	pampas grass
Poaceae	*Cynosurus echinatus* L.	bristly dogtail grass
Poaceae	*Dactylis glomerata* L.	orchard grass
Poaceae	*Deschampsia cespitosa* (L.) Beauv.	tufted hair-grass
Poaceae	*Elymus glaucus* Buckl.	blue wildrye
Poaceae	*Hierochloe occidentalis* Buckl.	California sweetgrass
Poaceae	*Holcus lanatus* L.	velvet grass
Poaceae	*Hordeum sp.* L.	barley
Poaceae	*Leymus ×vancouverensis* (Vasey) Pilger (pro sp.) *[mollis × triticoides]*	wildrye
Poaceae	*Lolium perenne* L.	English ryegrass
Poaceae	*Phalaris sp.* L.	canarygrass
Poaceae	*Phleum pratense* L.	common timothy
Polemoniaceae	*Navarretia squarrosa* (Eschsch.) Hook & Arn.	skunkweed
Polygonaceae	*Rumex acetosella* L.	common sheep sorrel
Polygonaceae	*Rumex crispus* L.	yellow dock
Polypodeaceae	*Adiantum pedatum* L.	northern maidenhair fern
Portulaceae	*Claytonia perfoliata* Donn ex Willd.	miner's lettuce
Portulaceae	*Claytonia sibirica* L.	Siberian candyflower
Primulaceae	*Trientalis borealis* Raf. ssp. *latifolia* (Hook.) Hultén	broadleaf starflower

Appendix A. Vascular plant species found in study location. Nomenclature follows the USDA PLANTS Database (USDA, 2007; continued).

Family	Species	Common name
Pteridaceae	*Pentagramma triangularis* (Kaulfuss) Yatskievych, Windham & Wollenweber	goldenback fern
Pyrolaceae	*Pyrola picta* Sm.	white-veined wintergreen,
Ranunculaceae	*Ranunculus californicus*	buttercup
Rhamnaceae	*Ceanothus thyrsiflorus* Eschsch.	blue blossom
Rhamnaceae	*Rhamnus californica* Eschsch.	coffeeberry
Rhamnaceae	*Rhamnus purshiana* (DC.) Cooper	cascara buckthorn
Rosaceae	*Fragaria vesca* L.	woodland strawberry
Rosaceae	*Heteromeles arbutifolia* (Lindl.) M. Roemer	toyon
Rosaceae	*Holodiscus discolor* (Pursh) Maxim.	oceanspray
Rosaceae	*Oemleria cerasiformis* (Hook & Arn.) J.W. Landon	oso berry
Rosaceae	*Prunus emarginata* (Hook.) Walp.	bitter cherry
Rosaceae	*Rosa californica* Cham. & Schldl.	California rose
Rosaceae	*Rosa gymnocarpa* Nutt.	wood rose
Rosaceae	*Rubus discolor* Focke	himalayan blackberry
Rosaceae	*Rubus parviflorus* Nutt.	thimbleberry
Rosaceae	*Rubus spectabilis* Pursh	salmonberry
Rosaceae	*Rubus ursinus* Cham. & Schlecht.	California blackberry
Rubiaceae	*Galium aparine* L.	common bedstraw
Salicaceae	*Salix hookeriana* Barratt ex Hook.	dune willow
Salicaceae	*Salix scouleriana* Barratt ex Hook.	Scouler's willow
Salicaceae	*Salix sitchensis* Sanson ex Bong.	Sitka willow
Salicaceae	*Salix sp*. L.	willow
Saxifragaceae	*Tolmiea menziesii* (Pursh) Torr. & Gray	pig-a-back plant
Scrophulariaceae	*Scrophularia californica* Cham. & Schlecht.	California bee-plant
Scrophulariaceae	*Veronica americana* Schwein. ex Benth.	water speedwell
Urticaceae	*Urtica dioica* L.	stinging nettle
Violeaceae	*Viola sp*. L.	violet

Appendix B. Transformed divergence values for vegetation classes by image type. Vegetation codes are defined in Table 5.

Class	A-Uc-Ld	Pm	Pm-Uc	Pm-Ag	Ld -UcPm	IPG	P
(1) Spectral separation for the aerial photo (0.15 m, 4-band)							
A-Uc-Ld	0						
Pm	133	0					
Pm-Uc	120	83	0				
Pm-Ag	134	23	33	0			
Ld-Uc-Pm	149	136	102	97	0		
IPG	1261	1029	991	999	698	0	
P	227	176	350	258	288	1112	0
(2) Spectral separation for the Quickbird image (0.61 m, 4-band)							
A-Uc-Ld	0						
Pm	224	0					
Pm-Uc	59	112	0				
Pm-Ag	160	27	69	0			
Ld-Uc-Pm	177	99	71	113	0		
IPG	1606	1345	1483	1530	1196	0	
P	934	395	740	493	632	1419	0
(3) Spectral separation for the NAIP image (1.0 m, 3-band)							
A-Uc-Ld	0						
Pm	119	0					
Pm-Uc	40	56	0				
Pm-Ag	122	23	31	0			
Ld-Uc-Pm	224	198	297	299	0		
IPG	489	548	650	695	137	0	
P	644	310	589	452	386	741	0